
ENSEMBLE-MIX: ENHANCING SAMPLE EFFICIENCY IN MULTI-AGENT RL USING ENSEMBLE METHODS

Tom Danino

The Andrew and Erna Viterbi Faculty of
Electrical & Computer Engineering
Technion- Israel Institute of Technology
tdanino12@gmail.com

Nahum Shimkin

The Andrew and Erna Viterbi Faculty of
Electrical & Computer Engineering
Technion- Israel Institute of Technology
shimkin@ee.technion.ac.il

ABSTRACT

Multi-agent reinforcement learning (MARL) methods have achieved state-of-the-art results on a range of multi-agent tasks. Yet, MARL algorithms typically require significantly more environment interactions than their single-agent counterparts to converge, a problem exacerbated by the difficulty in exploring over a large joint action space and the high variance intrinsic to MARL environments. To tackle these issues, we propose a novel algorithm that combines a decomposed centralized critic with decentralized ensemble learning, incorporating several key contributions. The main component in our scheme is a selective exploration method that leverages ensemble kurtosis. We extend the global decomposed critic with a diversity-regularized ensemble of individual critics and utilize its excess kurtosis to guide exploration toward high-uncertainty states and actions. To improve sample efficiency, we train the centralized critic with a novel truncated variation of the TD(λ) algorithm, enabling efficient off-policy learning with reduced variance. On the actor side, our suggested algorithm adapts the mixed samples approach to MARL, mixing on-policy and off-policy loss functions for training the actors. This approach balances between stability and efficiency and outperforms purely off-policy learning. The evaluation shows our method outperforms state-of-the-art baselines on standard MARL benchmarks, including a variety of SMAC II maps.

Keywords Multi-agent, Reinforcement learning, Ensemble learning, Selective exploration

1 Introduction

In recent years, *centralized training with decentralized execution* (CTDE) [1] algorithms have achieved state-of-the-art performance on various benchmark tasks [2, 3], emerging as a highly challenging yet promising area of research. In CTDE, the sharing of learning parameters and information between agents is enabled during training, while in execution time, agents are deployed in a fully decentralized manner. Value decomposition algorithms play a crucial role in the success of CTDE. This family of algorithms suggests decomposing the global value function into individual per-agent components via a centralized mixing network, enabling agents to learn and coordinate their actions within a team more efficiently. The idea has also been extended to multi-agent policy gradient (MAPG) frameworks [4, 5], where the global critic is decomposed into individual Q functions, resulting in significant performance gains. Despite this progress, both approaches remain susceptible to the curse of dimensionality [6], which inflicts longer training times and hinders effective exploration due to the large joint action space. This challenge is further exacerbated by the increased variance common in MARL settings due to potentially suboptimal and exploratory behaviors of multiple agents [4]. Such conditions can lead to amplified errors in the Bellman backup process and destabilize learning [7].

Our work comprises these three tightly connected challenges: selective exploration, coping with high variance updates, and enhancing sample efficiency. We introduce a novel MAPG algorithm named Ensemble-MIX that includes improvements in all three domains.

The first component of Ensemble-MIX deals with selective exploration based on ensemble kurtosis. We propose an approach where each agent leverages the excess kurtosis of its critic’s ensemble to identify high-uncertainty actions

and prioritizes them during action selection. We employ an ensemble approach (Fig. 1) since ensemble variability is a good indicator of uncertainty with demonstrated sample-efficiency properties in both single-agent and multi-agent scenarios [8, 9]. Rather than relying on ensemble variance, we propose using ensemble kurtosis due to its higher sensitivity to outliers, which helps address efficiency limitations, as further discussed in Section 4. While kurtosis has been previously proposed as a measure of uncertainty in other fields [10, 11], to the best of our knowledge, this is its first application within the RL domain. To ensure minimal ensemble overhead, we also propose promoting diversity among ensemble members via a regularization method based on the Bhattacharyya distance. Prior studies have shown that ensemble members often converge to similar solutions, suggesting that facilitating diversity can improve overall performance while enabling the use of smaller ensembles [12, 13]. This strategy helps us limit parameter overhead without compromising effectiveness.

The second part of our work focuses on improving sample efficiency. We make two novel suggestions in this area. First, we extend the mixed actors approach [14] to the multi-agent setting. Leveraging off-policy data is appealing due to its superior sample efficiency compared to strictly on-policy methods. However, it comes with the risk of bias, as outdated samples may not accurately represent the current policy, potentially leading to unstable training. This trade-off between efficiency and stability is well-documented in single-agent RL [15, 14], and becomes even more pronounced in multi-agent environments due to the high dimensionality and inter-agent dependencies. We address this by combining on-policy and off-policy updates when training the actors, aiming to balance between stability and efficiency. In Section 5, we present a theoretical analysis showing that the bias in our gradient updates remains bounded. Second, we suggest a novel truncated version of TD(λ) that combines uncertainty estimation for training the critics. Our approach is more sample efficient than the tree backup (TB) critic used by DOP [4] while improving stability by accounting for the exploding importance sampling ratios and high variance samples that exist in multi-agent settings.

2 Background

Decentralised partially observable Markov decision processes (Dec-POMDPs). A Dec-POMDP [16] models the interaction between cooperative agents and a partially observable environment. It is represented by the tuple $\langle \mathcal{I}, \mathcal{S}, \mathcal{A}, \mathcal{P}, \Omega, \mathcal{O}, r, \gamma \rangle$, where \mathcal{I} denotes a finite set of k agents, and $s \in \mathcal{S}$ denotes the true state of the environment. Each agent selects an action $a_i \in \mathcal{A}$, forming the joint action space $\mathbf{a} = [a_i]_{i=1}^k \in \mathcal{A}$. $r(s, \mathbf{a})$ denotes the shared reward for executing the set of joint actions in the environment. Executing the set of actions results in a transition to the next state s' , according to the transition function $\mathcal{P}(\cdot | s, \mathbf{a})$. The Dec-POMDP considers partially observable settings where each agent i receives a partial observation $o_i \in \Omega$ according to the observation probability function $\mathcal{O}(o_i | s, a_i)$. The discount factor is denoted by $\gamma \in [0, 1)$ and the joint action-observation history of the set of agents is denoted by $\tau \in \mathcal{T}$. For a joint set of policies $\{\pi_i\}_{i=1}^k$ and corresponding learning parameters $\{\theta_i\}_{i=1}^k$, the parameterized policies are denoted by $\{\pi_{\theta_i}\}_{i=1}^k$. We use the notation $\bar{z}^i = f_{\theta_i}(\tau_i)$ to denote the logits of the i_{th} actor network before applying the softmax function. The set of behaviour policies are defined by $\{\mu_i\}_{i=1}^k$.

Value decomposition and monotonic constraints in multi-agent reinforcement learning. Value decomposition in MARL involves decomposing the overall state value function into individual per-agent value functions, enabling an efficient credit assignment by ensuring that agents receive rewards based on their specific contributions to the total cumulative reward. To ensure that maximizing the global Q function also maximizes the per-agent Q functions the Individual-Global-Maximum (IGM), condition must be enforced, which mean that each agent’s optimal individual action aligns with the joint action that maximizes the global value function.

Value-decomposition networks (VDN) express the global value function as the sum of individual Q -values. Maintaining additivity ensures IGM consistency and enables CTDE. QMIX enhances VDN by employing a centralized mixing network to represent Q_{tot} as a non-linear and monotonic combination of individual value functions.

MAPG architecture and loss functions. DOP [4] is an MAPG method that employs a centralized decomposed critic with decentralized actors (Figure 1). Since our design for the critic’s loss function draws inspiration from DOP, we bring the similar parts here for easier comparison. In DOP, the centralized critic is trained by minimizing the following loss:

$$\mathcal{L}_{\text{critics}}(\phi) = \mathbf{c}\mathcal{L}^{\text{on-TD}(\lambda)}(\phi) + (1 - \mathbf{c})\mathcal{L}^{\text{off-TB}}(\phi), \quad (1)$$

where \mathbf{c} is the tuning factor, used to balance between off-policy and on-policy updates. To construct the loss function two buffers are maintained: samples from the off-policy buffer yield $L^{\text{off-TB}}$, while $\mathcal{L}^{\text{on-TD}(\lambda)}$ is calculated with samples from the smaller on-policy buffer that stores only recent experiences. $\mathcal{L}_{\text{off}}(\phi)$ is defined as $\mathbb{E}_{\pi}[(y^{\text{off}} - Q_{\text{tot}}^{\phi}(\tau, \mathbf{a}))^2]$, and y^{off} is the tree backup update target, as suggested by [4, 17]:

$$y^{\text{off}} = Q_{\text{tot}}^{\phi'}(\tau, \mathbf{a}) + \sum_{t=0}^{m-1} \prod_{l=0}^t \lambda \pi(a_l | \tau_l) [r_t + \gamma \mathbb{E}_{\mathbf{a}_{t+1} \sim \pi} [Q_{\text{tot}}^{\phi'}(\tau_{t+1}, \mathbf{a}_{t+1})] - Q_{\text{tot}}^{\phi'}(\tau_t, \mathbf{a}_t)], \quad (2)$$

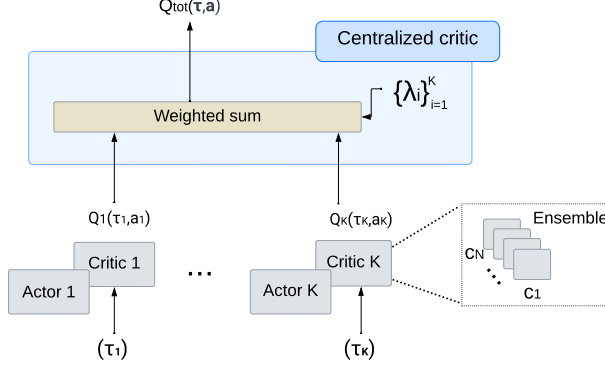


Figure 1: Ensemble-MIX architecture

where $\tau_0 = \tau$, $\mathbf{a}_0 = \mathbf{a}$. The target mixing network is denoted by $Q_{\text{tot}}^{\phi'}$ and the joint policy π is defined by the product of individual policies: $\pi(\mathbf{a}_l | \tau_l) = \prod_{i=1}^k \pi_i(a_i^l | \tau_i^l)$. In our paper, we use a similar expression to construct the joint behavior policy $\mu(\mathbf{a}_l | \tau_l)$. The full specification of the critic loss, along with details on other components, can be found in [4].

Kurtosis. The kurtosis of a random variable x is defined as the fourth standardized moment [18]:

$$\kappa[x] = \mathbb{E}\left[\left(\frac{x - \mu}{\sigma}\right)^4\right] = \frac{\mathbb{E}[(x - \mu)^4]}{(\mathbb{E}[(x - \mu)^2])^2}, \quad (3)$$

where σ denotes the standard deviation and μ the mean of the distribution. When measuring the kurtosis of N samples it is custom to use the excess kurtosis:

$$g_2(\{x_i\}_{i=1}^N) = \frac{\frac{1}{n} \sum_{i=1}^N (x_i - \bar{x})^4}{\left[\frac{1}{N} \sum_{i=1}^n (x_i - \bar{x})^2\right]^2} - 3, \quad (4)$$

where x_i is the i_{th} sample, \bar{x} denotes the samples mean, and 3 is the kurtosis of the normal distribution. In our work, each sample corresponds to a distinct ensemble member, and $\kappa_{Q_i^{\phi_i}}(\tau_i, a_i) = g_2(\{Q^{\phi_{i,j}}(\tau_i, a_z)\}_{j=1}^N)$ denotes the i_{th} critic ensemble's predictions for action a_i . Note that the kurtosis indicates the distribution's tails and the presence of outliers within it. Subtracting the constant 3 sets the normal distribution as a reference point. Previous works from other domains made a similar use of the normal distribution to estimate the excess kurtosis. For instance, [19] estimated value at risk (VaR) in financial time series using excess kurtosis, measuring it relatively to the normal distribution. [20] applied kurtosis for outlier detection in financial time series and used excess kurtosis as a criterion for portfolio selection.

Variance in multi-agent RL. Variance in RL typically refers to the variability in rewards received by an agent as it interacts with the environment. It is a measure of how much the actual rewards obtained by the agent deviate from the expected or average reward. High variance can lead to inconsistent and unstable learning, making it difficult for the agent to converge to an optimal policy or value function. This issue is further exacerbated in multi-agent settings, as MARL methods suffer from higher variance during training compared to their single-agent counterpart [21]. Unlike single-agent settings, where the variance of an individual agent usually stems only from randomness in the reward or the environment, in multi-agent settings, both suboptimally and exploration of other agents induce variance. The focus of this work is on centralized training methods, where variance propagates between agents through the centralized critic/mixing network. As a result, $\text{Var}[Q_{\text{tot}}]$ can become very large. For instance, assuming a linearly decomposed critic, denoted by $Q_{\text{tot}}^{\phi}(\tau, \mathbf{a}) = \sum_i \lambda_i(\tau) Q_i^{\phi_i}(\tau_i, a_i)$, its variance $\text{Var}_{\mathbf{a} \sim \pi}[Q_{\text{tot}}^{\phi}(\tau, \mathbf{a})]$, can be expressed as follows:

$$\text{Var}_{a_1 \sim \pi_1, \dots, a_k \sim \pi_k} [\lambda_1 Q_1^{\phi_1}(\tau_1, a_1) + \dots + \lambda_k Q_k^{\phi_k}(\tau_k, a_k)]. \quad (5)$$

It can be seen that the variance of Q_{tot} depends on the actions taken by all the agents and their individual Q -functions. Since Q_{tot} is backpropagated back to all critics, each agent is exposed to variance induced by the other agents.

3 Related Work

Several methods integrated MAPG architectures with value decomposition. DOP [4] proposed a decomposed shared critic that improves sample efficiency by combining on-policy and off-policy loss functions to train the critic. PAC

[5] suggested an off-policy actor-critic with assistive information to enhance learning. [22] addressed efficiency in MARL by grouping agents before the decomposition process to enable a more efficient collaboration. Exploration in MARL has also been addressed in several works. [23] suggested collaborative and efficient exploration by guiding the agents to explore only meaningful states. [5] added an entropy term to the central critic with a decaying temperature to avoid over-exploration. [24] suggested efficient exploration via dynamically adjusted entropy temperature that performs more exploration when higher return is expected. Diversity in ensembles has been mainly addressed in single-agent RL. These include maximizing inequality measures (e.g., the Theil index) [13], using random initialization of learning parameters, and training ensemble members on different sample sets [7].

4 Ensemble MIX

This section presents Ensemble-MIX, our combined algorithm to enhance sample efficiency and enable selective exploration. Our framework comprises 4 main components: (1) Truncated TD(λ) loss for learning Q_{tot} based on uncertainty estimation, (2) actors trained with mixed off-and-on loss functions, (3) selective exploration through kurtosis-based prioritization, and (4) diversity regularization within the ensemble based on Bhattacharyya distance.

4.1 MAPG architecture with mixed actors and uncertainty weighting

In our scheme, each individual critic i is composed of an ensemble of N sub-critics (Fig. 1):

$$Q_i^{\phi_i}(\boldsymbol{\tau}, a_i) = \frac{1}{N} \sum_{j=1}^N Q_i^{\phi_{i,j}}(\tau_i, a_i). \quad (6)$$

The mean Q -value of the i_{th} agent is denoted by $Q_i^{\phi_i}$, while each member in the ensemble is denoted by $Q_i^{\phi_{i,j}}$. The global Q -function is decomposed into a linear combination of individual functions, as proposed by several previous works [4, 25]:

$$Q_{tot}^{\phi}(\boldsymbol{\tau}, \mathbf{a}) = \sum_{i=1}^K \lambda_i(\boldsymbol{\tau}) Q_i^{\phi_i}(\tau_i, a_i) + b(\boldsymbol{\tau}), \quad (7)$$

with K denotes the number of agents. To maintain the monotonic constraint, as suggested by QMIX, the mixing network coefficients λ_i are restricted to be positive. Q_{tot} also includes a learnable bias, denoted by b .

Uncertainty weighted decomposed critic. Our scheme for the critic loss is motivated by DOP [4], which showed TD(λ) to be highly effective in CTDE settings. However, in DOP, the critic efficiency is compromised by its use of the tree backup (TB) which applies the $\lambda\pi(\mathbf{a}|\boldsymbol{\tau})$ coefficient (Eq. 2). Such an approach unnecessarily cuts the traces in the near on-policy case, hindering effective use of the training data [17]. Standard methods from single-agent RL that cope with this problem, such as the retrace(λ) algorithm [17] aren't well-suited to multi-agent settings. Retrace balances efficiency and variance by setting the coefficient as $\min(1, \frac{\pi(\mathbf{a}|\boldsymbol{\tau})}{\mu(\mathbf{a}|\boldsymbol{\tau})})$. The effectiveness of this technique is reduced in MARL since the importance sampling (IS) ratio can grow exponentially with the number of agents [4], leading to many traces being indiscriminately truncated to 1 regardless of discrepancies from the current policy.

To address this problem, we propose a novel variation of TD(λ) that truncates the IS ratio using an uncertainty-based score which quantifies how much the ensemble of critics is uncertain about the chosen action. The choice for this weighting is motivated by the fact that in our scheme, both the critics and the actors are trained using the same mix of on-policy and off-policy samples, making the critics more suitable to cut unlikely traces. Note that uncertainty weighting serves an additional purpose in this case, as it down-weights the contribution of noisy and high variance updates that the presence of multiple agents induces on the system (Sec. 2). A discussion of the types of uncertainty in MARL environments and the use of ensembles for detection is given in Appendix E. Additionally, to verify the effectiveness of our approach, an ablation study comparing our technique to TB and retrace(λ) is given in Figs. 3 and 5. At the first step, we quantify uncertainty for each agent by employing the kurtosis of the ensemble. Kurtosis is considered more sensitive than variance in terms of outlier detection [18], as it allows for more variability around the mean while punishing positive excess-tailedness (outliers). To obtain a bounded score, we adopt the weight function proposed by [7]:

$$w_i(\tau_i, a_i) = 0.5 + \mathcal{S}(-C_1 \kappa_{Q_i^{\phi_i}}(\tau_i, a_i)), \quad (8)$$

replacing variance with kurtosis. $\mathcal{S} : \mathbb{R} \rightarrow (0, 1)$ denotes the sigmoid function, and $\kappa_{Q_i^{\phi_i}}(\tau_i, a_i)$ is the kurtosis of the i_{th} critic ensemble's predictions for action a_i . C_1 is a scaling factor. Note that the kurtosis remains positive, as it is not computed relative to the normal distribution, and no subtraction of 3 takes place, ensuring that $\frac{1}{2} \leq w_i(\tau_i, a_i) \leq 1$. The

weighted uncertainty of the entire team of agents is denoted by:

$$w(\boldsymbol{\tau}, \mathbf{a}) = \frac{\sum_{i=1}^k \lambda_i(\boldsymbol{\tau}) w_i(\tau_i, a_i)}{\sum_{i=1}^k \lambda_i(\boldsymbol{\tau})}. \quad (9)$$

Next, we define the critic loss. Our architecture is built on DOP [4], as similar to them, we train the centralized critic by combining off-policy and on-policy loss functions:

$$\mathcal{L}_{\text{critics}}(\phi) = \mathbf{c}\mathcal{L}^{\text{on}}(\phi) + (1 - \mathbf{c})\mathcal{L}^{\text{off}}(\phi), \quad (10)$$

where \mathbf{c} is the relative scaling factor, used to balance between off-policy and on-policy updates. To construct the loss function two buffers are maintained: samples from the off-policy buffer yield L^{off} , while \mathcal{L}^{on} is calculated with samples from the smaller on-policy buffer that stores only recent experiences. The novelty in our critic, compared to DOP, stems from the change in \mathcal{L}^{off} . Instead of scaling the loss proportionally to $\lambda\pi(\mathbf{a}, \boldsymbol{\tau})$, we apply our proposed truncated IS ratio the combines uncertainty weighting:

$$y^{\text{off}} = Q_{\text{tot}}^{\phi'}(\boldsymbol{\tau}, \mathbf{a}) + \sum_{t=0}^{m-1} (\gamma\lambda)^t C_{\boldsymbol{\tau}} [r_t + \gamma \mathbb{E}_{\mathbf{a}_{t+1} \sim \pi} [Q_{\text{tot}}^{\phi'}(\boldsymbol{\tau}_{t+1}, \mathbf{a}_{t+1})] - Q_{\text{tot}}^{\phi'}(\boldsymbol{\tau}_t, \mathbf{a}_t)], \quad (11)$$

where $C_{\boldsymbol{\tau}} = \prod_{l=0}^t \min(w(\boldsymbol{\tau}_l, \mathbf{a}_l), \frac{\pi(\mathbf{a}_l | \boldsymbol{\tau}_l)}{\mu(\mathbf{a}_l | \boldsymbol{\tau}_l)})$. The multiplicative approach is similar to traditional techniques [17], which multiply the coefficients up to the current time t . Note that since w is bounded, it can also be seen as a subtraction of an uncertainty bonus ϵ from 1, i.e., $w(\boldsymbol{\tau}_l, \mathbf{a}_l) = 1 - \epsilon$. The overall off-policy loss is calculated as $\mathcal{L}^{\text{off-TB}}(\phi) = \mathbb{E}_{\beta}[(y^{\text{off}} - Q_{\text{tot}}^{\phi}(\boldsymbol{\tau}, \mathbf{a}))^2]$.

The on-policy loss is defined as $\mathcal{L}^{\text{on}}(\phi) = \mathbb{E}_{\pi}[(y^{\text{on}} - Q_{\text{tot}}^{\phi}(\boldsymbol{\tau}, \mathbf{a}))^2]$, with the standard TD(λ) target:

$$y^{\text{on}} = Q_{\text{tot}}^{\phi'}(\boldsymbol{\tau}, \mathbf{a}) + \sum_{t=0}^{\infty} (\gamma\lambda)^t [r_t + \gamma Q_{\text{tot}}^{\phi'}(\boldsymbol{\tau}_{t+1}, \mathbf{a}_{t+1}) - Q_{\text{tot}}^{\phi'}(\boldsymbol{\tau}_t, \mathbf{a}_t)], \quad (12)$$

Mixed on-policy off-policy actors. Previous MAPG and value decomposition approaches either trained the actors in an on-policy [4] or off-policy manner [5]. To improve existing schemes and enable sample-efficient actors with lower bias, we propose training the actors by combining gradients from on and off loss functions [14]:

$$D_{\nu}^{\beta}(\pi_i, \pi_{-i}) = (1 - \nu)\mathbb{E}_{\rho^{\pi}, \pi_i} [\nabla_{\theta_i} \log \pi_i(a_i | \tau_i; \theta_i) U_{\pi_i}^{\phi_i}(\tau_i, a_i)] + \nu\mathbb{E}_{\rho^{\beta}} [\nabla_{\theta_i} \bar{Q}_{\text{tot}}^{\phi}(\boldsymbol{\tau}, (a_i, \mathbf{a}_{-i}))],$$

where $\bar{Q}_{\text{tot}}^{\phi}(\boldsymbol{\tau}, (a_i, \mathbf{a}_{-i})) = \mathbb{E}_{\pi_i} [Q_{\text{tot}}^{\phi}(\boldsymbol{\tau}, (a_i, \mathbf{a}_{-i}))]$, and ν is the relative scaling factor. The joint off-policy is denoted by $\beta(\mathbf{a} | \boldsymbol{\tau}) = \prod_{i=1}^k \beta_i(a_i, \tau_i)$, and ρ^{β} is the joint off-policy state distribution. U_i is the advantage function [4]:

$$U_i^{\phi_i}(\tau_i, a_i) = \lambda_i(\boldsymbol{\tau}) (Q_i^{\phi_i}(\tau_i, a_i) - \sum_{x \in \mathcal{A}} \pi_{\theta_i}(x | \tau_i) Q_i^{\phi_i}(\tau_i, x)). \quad (13)$$

Combining both approaches is known to produce good results [14] in single-agent RL with higher stability compared to off-policy training. In Sec. 5, we present a theoretical analysis showing that the bias in our gradient Updates remain bounded.

4.2 Exploration based on ensemble kurtosis

Standard exploration techniques from the single-agent domain, like entropy maximization [26], may result in excessive and inefficient exploration when applied to multi-agent settings, potentially degrading performance [24]. This is because such methods encourage agents to explore as randomly as possible [27], visiting redundant states in the process [23]. To address this limitation, we propose leveraging ensemble kurtosis to adjust the level of exploration and prioritize actions associated with higher kurtosis values. Our algorithm applies kurtosis in a twofold manner. First, each agent detects high-uncertainty states based on the mean value of the kurtoses taken over all actions in the action space. Second, once a relevant state is detected, prioritization is applied by weighting actions according to their kurtosis. In each iteration of action selection, every i_{th} agent calculates the kurtosis over all M_i actions:

$$\bar{g}_i(\tau_i, \{Q^{\phi_{i,j}}\}_{j=1}^N) = \frac{\sum_{z=1}^{M_i} g_2(\{Q^{\phi_{i,j}}(\tau_i, a_z)\}_{j=1}^N)}{M_i}, \quad (14)$$

where g_2 is the excess kurtosis described in Eq. 4. If $\bar{g}_i > 0$ then an exploration step is performed by adding the kurtosis of each action to the corresponding logits, otherwise, a standard action selection is executed. Conditioning on

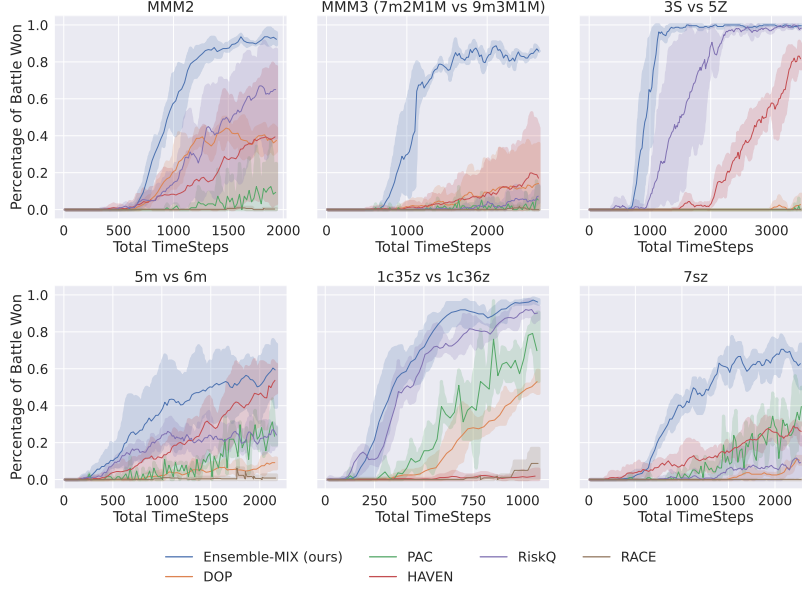


Figure 2: Results on the SMAC benchmark

the positivity of \bar{g}_i guarantees exploration is performed only on areas of positive excess kurtosis, Formally, given the M_i logits of actor i on a given state, denoted by $\bar{z}^i = \{z_1^i, \dots, z_{M_i}^i\}$, and the corresponded ensemble kurtosis, denoted by $\{\kappa_{Q_i^{\phi_i}}(\tau_i, a_1), \dots, \kappa_{Q_i^{\phi_i}}(\tau_i, a_{M_i})\}$, then the j th weighted logit of actor i is given by:

$$\tilde{z}_j^i = \begin{cases} z_j^i + \beta \kappa_{Q_i^{\phi_i}}(\tau_i, a_j), & \text{if } g_i > 0 \\ z_j^i, & \text{otherwise} \end{cases} \quad (15)$$

where β is a hyperparameter, chosen to be sufficiently small so as not to dominate the value of \tilde{z}_j^i . Similarly to standard actor-critic algorithms, the softmax operator is applied to the weighted logits to create a distribution for action selection. The complete algorithm is provided in Appendix A. Note that prior to our work, [7, 28] suggested leveraging ensemble variance as an exploration bonus. In section 7 we discuss the difference between the two approaches, emphasizing efficiency improvement, which is especially crucial for successful exploration in multi-agent settings.

4.3 Diversity in ensemble via Bhattacharyya regularization

Previous works from the single agent domain showed that encouraging diversity in ensemble can dramatically reduce the size of the ensemble. To this end, we propose utilizing the Bhattacharyya distance as a regularization term. Bhattacharyya distance is widely used in classification and clustering tasks due to its ability to measure distributional overlap [29]. To our knowledge, there have been no prior efforts to apply the Bhattacharyya distance in the context of RL, despite studies indicating it to be more stable than other similarity measures such as KL divergence [30]. The Bhattacharyya term is calculated as the sum of distances between the mean Q -function of the ensemble $Q_i^{\phi_i}$ and all the distinct Q -functions:

$$\delta_{B_{\text{total}}}^{Q_i}(\tau_i) = \sum_{j=1}^N \delta_B \left(\sigma \left(Q_i^{\phi_i}(\tau_i, \cdot) \right), \sigma \left(Q_i^{\phi_{i,j}}(\tau_i, \cdot) \right) \right). \quad (16)$$

The sum extends over all members within the ensemble while σ denotes the soft-max function. The distance δ_B is given by [31]:

$$\delta_B \left(\sigma \left(Q_i^{\phi_i}(\tau_i, \cdot) \right), \sigma \left(Q_i^{\phi_{i,j}}(\tau_i, \cdot) \right) \right) = -\ln \left(\sum_{a \in \mathcal{A}} \sqrt{\sigma(Q_i^{\phi_i}(\tau_i, a)) \sigma(Q_i^{\phi_{i,j}}(\tau_i, a))} \right).$$

The regularization term is added to the critic's loss with a negative sign:

$$\mathcal{L}_{\text{total}}(\phi) = \mathcal{L}_{\text{critics}}(\phi) - C_2 \sum_{i=1}^K \delta_{B_{\text{total}}}^{Q_i}(\tau_i). \quad (17)$$

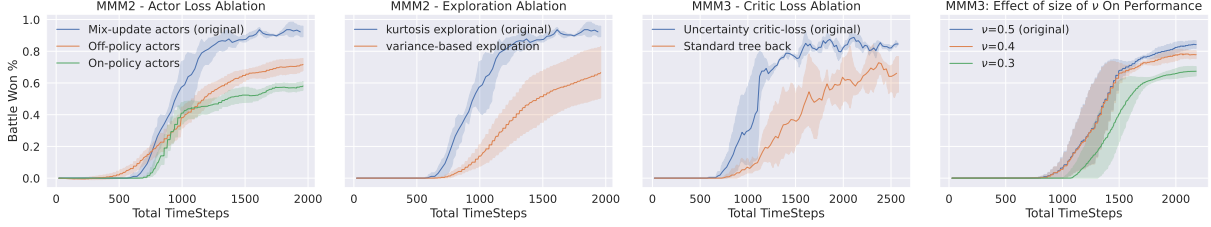


Figure 3: Ablation study on MMM2 and MMM3 maps for critic loss, actor loss, and exploration mechanism. Analysis on different values of ν is presented in the right figure.

To prevent $\delta_{B_{\text{total}}}^{Q_i}$ from dominating the loss function, we set C_2 to be sufficiently small (see Appendix B).

5 Bounds on the Bias of Mixed Actors

In this section, we bound the bias of the gradient update for each individual agent. Since each agent independently updates its policy, analyzing the bias on a per-agent basis is more intuitive. To do so, we first define the true Q -function of the i_{th} agent [4]:

$$Q_i^\pi(\tau, a_i) = \sum_{\mathbf{a}^{-i}} \pi_{-i}(\mathbf{a}^{-i}|\tau_{-i}) Q_{\text{tot}}^\pi(\tau, (\mathbf{a}_i, \mathbf{a}^{-i})), \quad (18)$$

and the corresponding gradient update:

$$\nabla_{\theta_i} J(\pi_i, \pi_{-i}) = \mathbb{E}_{\tau \sim \rho^\pi, \mathbf{a}_i \sim \pi_i} [\nabla_{\theta_i} \log \pi_i(a_i|\tau_i; \theta_i) Q_i^\pi(\tau, a_i)], \quad (19)$$

where $\pi_{-i}(\mathbf{a}^{-i}|\tau_{-i}) = \prod_{j \neq i} \pi_j(a_j|\tau_j)$. We denote the discrepancy between the true Q -function and the approximated function of the i_{th} agent by:

$$Q_{\phi_i}^\pi(\tau, a_i) = Q_i^\pi(\tau, a_i) - \lambda_i(\tau) Q_i^{\phi_i}(\tau_i, a_i). \quad (20)$$

The bias can then be bound by estimating the difference between the gradient of the true objective $\nabla_{\theta_i} J(\pi_i, \pi_{-i})$ and the mixed gradient update $D_\nu^\beta(\pi_i, \pi_{-i})$ we use in the paper.

Proposition 1. Let the maximal KL divergence between two policies π, β be denoted by $D_{\text{max}}^{\text{KL}}(\pi, \beta) = \max_{\tau} D_{\text{KL}}(\pi(\cdot|\tau), \beta(\cdot|\tau))$, and let $\omega_1 = \max_{\tau, \mathbf{a}} \left\| \nabla_{\theta_i} \log(\pi_i(a_i|\tau_i; \theta_i)) \lambda_i(\tau) Q_{\phi_i}^\pi(\tau, a_i) \right\|_1$, $\omega_2 = \max_{\tau} \left\| \nabla_{\theta_i} \lambda_i(\tau) \mathbb{E}_{\pi_i} [Q_i^{\phi_i}(\tau_i, a_i)] \right\|_1$. Then, the learning bias of each agent can be bounded as follows:

$$\left\| \nabla_{\theta_i} J(\pi_i, \pi_{-i}) - D_\nu^\beta(\pi_i, \pi_{-i}) \right\|_1 \leq \frac{\omega_1}{1-\gamma} + \frac{2\omega_2\nu\gamma}{(1-\gamma)^2} \sqrt{D_{\text{max}}^{\text{KL}}(\pi, \beta)}. \quad (21)$$

The bound tells us that the bias of each agent’s gradient update depends on two main factors: errors in the approximation of Q_i^π , as measured by $Q_{\phi_i}^\pi$, and second, how much the joint on-policy diverge from the (joint) policy used to collect the off-policy data (similarly to the bound in the single agent case [14]). A detailed proof is given in Appendix G.

6 Experiments and Results

The objective of the empirical evaluation is to assess the performance of our approach. We measure and compare the percentage of battle wins or total reward of the team of agents across several standard benchmarks: Starcraft II [32], multi-agent car following (MACF) [33], and predator prey (PP) [5]. The hyperparameters and network architecture are fixed for all of the experiments, full specification is given in Appendix B. We use 4 different seeds for each experiment, adopting a 95% confidence interval. A comparison is conducted between our approach and DOP, HAVEN [34], PAC, RiskQ [33], and RACE [35]. We set the size of the ensemble to be $N = 10$. Each critic in the ensemble is implemented with a fully connected 2 layers network. Further explanation on the SMAC maps used in our experiments is provided in Appendix C.

Performance evaluation (SMAC). Figure 2 presents the total score throughout the training process in 6 SMAC maps. The shaded areas around the learning curves represent the standard deviation. All measurements are taken as follows: every T steps the training process is paused and a fixed number of U testing episodes is executed. The mean score over the test episodes is recorded and used in the graphs. To maintain a decentralized execution, in test time the actors in

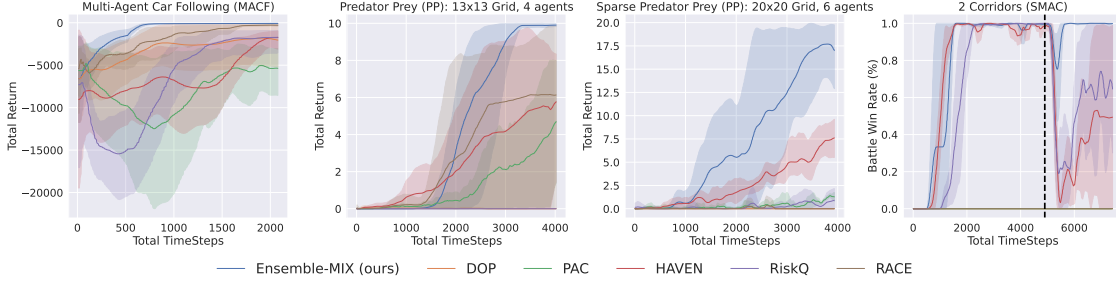


Figure 4: Results on predator-prey, MACF, and 2 corridors map (SMAC)

our method execute a standard softmax policy, without the ensemble kurtosis added to the logits. Fig. 2 shows that Ensemble-MIX outperforms all other methods on the tested SMAC maps. We specifically excel in the MMM2 and MMM3, which are considered extremely challenging and categorized as super-hard. Note that those are maps that pose challenges such as diversity among agents; RiskQ and HAVEN achieved second and third best performance on those maps, attributed to hierarchical reward design and distributional Q-function mechanism, which support diverse strategies. DOP, an older method, generally underperformed compared to other baselines, except on the MMM maps. This result can be partially explained by DOP utilization of softmax policies, which enable greater stochasticity and may promote more diverse behavior.

2 corridors and predator prey. To show that our method performs effective exploration, we conduct additional experiments with the 2 corridors map [36] and PP. In the 2 corridors, 2 allies fight an enemy unit with the shorter corridor closed mid-training (dotted line in Fig. 4). This requires the agents to explore the terrain and learn how to use the second corridor when attacking the enemy unit. The results show that our method adapts to the change faster than the baseline methods while achieving the best overall results. In PP, we construct settings with a larger grid, where 4 agents have to be involved in every catch. This makes catching prey and rewards much more sparse than in the default settings. Both HAVEN and Ensemble-MIX achieved good results in PP, specifically in the larger grid, where state exploration is required and the other methods underperformed.

MACF. In MACF (Fig. 4), two cars follow each other, with the aim of collaboratively reaching the goal. This is a stochastic environment that introduces risk [33] due to potentially stochastic catastrophic events. We use this setting to verify the effectiveness of our uncertainty weighting when aleatoric noise is present in the environment.

7 Discussion

Computation requirements. All experiments are conducted with an ensemble of size $N = 10$. Achieving good performance with a relatively small value of N is made possible due to the diversity regularization we apply via the Bhattacharyya distance. This finding is consistent with previous studies that show diversity among members of the ensemble can reduce the size of N from a few hundred to less than a few dozen [12, 13]. Yet, the use of the ensemble technique introduces additional overhead during training due to additional parameters.

Comparison to previous works. Prior to our work, [7, 28] suggested leveraging ensemble variance as an exploration bonus for Q -learning algorithms. Applying it directly to actor-critic and multi-agent settings yields suboptimal performance, as demonstrated in our ablation studies. Our approach differs from [28] by incorporating excess kurtosis and selectively applying it as exploration bonuses. This ensures that agents do not always engage in exploration and maintain higher efficiency, which becomes critical as the joint action space grows with the number of agents.

7.1 Ablation study and parameter analysis

This section presents the main ablation results. The complete graphs with full parameter analysis are given in Appendix F.

Variance versus kurtosis for exploration (Fig. 3). We validate the effect of kurtosis for exploration (Eq. 15) by comparing it to the original algorithm suggested by [7, 28]. In [7], instead of applying exploration bonuses only to high-uncertainty states that correspond to positive excess kurtosis, the variance is added to in all time steps, regardless of the level of uncertainty.

Actors loss and off-policy samples. To evaluate the impact of training actors using a mix of off-policy and on-policy samples we compare three approaches: training the actors solely with on-policy samples, training with off-policy samples, and a mix of off-policy and on-policy. Results for the MMM2 map are shown in Fig. 3.

Critic loss. The ablation compares our truncated TD(λ) technique to the original TB critic of DOP (Fig. 3) and the

retrace algorithm (Fig. 5).

Parameter analysis. Fig. 3 shows experiments with different values of ν on MMM3. Additional parameter analysis for β , C_1 , c and different ensemble sizes is given in the appendix.

8 Conclusion

This paper presented Ensemble-MIX, a novel MAPG algorithm aiming to enhance sample efficiency in MARL settings and perform selective exploration via uncertainty quantification. Our technique for selective exploration leverages ensemble excess kurtosis to guide the visitation of high-uncertainty states and actions. When training the shared critic, we support both sample efficiency and variance reduction by suggesting a truncated version of the TD(λ) algorithm that incorporates ensemble uncertainty into the weighting function. By training the actors with a combination of on-policy and off-policy loss functions, our method achieves both sample efficiency and higher stability in comparison to relying solely on off-policy learning. We also highlight the importance of ensemble diversity to reducing parameter overhead, introducing a simple approach to enhance diversity using Bhattacharyya regularization. Experimental results show that Ensemble-MIX achieves state-of-the-art performance on several benchmarks, including StarCraft II, and generalizes well to scenarios with homogeneous or heterogeneous agents, even when their action spaces differ.

References

- [1] Tabish Rashid, Gregory Farquhar, Bei Peng, and Shimon Whiteson. Weighted qmix: Expanding monotonic value function factorisation for deep multi-agent reinforcement learning. *Advances in neural information processing systems*, 33:10199–10210, 2020.
- [2] Georgios Papoudakis, Filippos Christianos, Lukas Schäfer, and Stefano V Albrecht. Benchmarking multi-agent deep reinforcement learning algorithms in cooperative tasks. *arXiv preprint arXiv:2006.07869*, 2020.
- [3] Yongsheng Mei, Hanhan Zhou, and Tian Lan. Projection-optimal monotonic value function factorization in multi-agent reinforcement learning. In *Proceedings of the 2024 International Conference on Autonomous Agents and Multiagent Systems*, 2024.
- [4] Yihan Wang, Beining Han, Tonghan Wang, Heng Dong, and Chongjie Zhang. Dop: Off-policy multi-agent decomposed policy gradients. In *International conference on learning representations*, 2020.
- [5] Hanhan Zhou, Tian Lan, and Vaneet Aggarwal. Pac: Assisted value factorization with counterfactual predictions in multi-agent reinforcement learning. *Advances in Neural Information Processing Systems*, 35:15757–15769, 2022.
- [6] Wei Du and Shifei Ding. A survey on multi-agent deep reinforcement learning: from the perspective of challenges and applications. *Artificial Intelligence Review*, 54(5):3215–3238, 2021.
- [7] Kimin Lee, Michael Laskin, Aravind Srinivas, and Pieter Abbeel. Sunrise: A simple unified framework for ensemble learning in deep reinforcement learning. In *International Conference on Machine Learning*, pages 6131–6141. PMLR, 2021.
- [8] Xinyue Chen, Che Wang, Zijian Zhou, and Keith W. Ross. Randomized ensembled double q-learning: Learning fast without a model. In *International Conference on Learning Representations*, 2021.
- [9] Agent Reinforcement Learning. Ensemble value functions for efficient exploration in multi-agent reinforcement learning.
- [10] Jon Anda, Alexander Golub, and Elena Strukova. Economics of climate change under uncertainty: Benefits of flexibility. *Energy Policy*, 37(4):1345–1355, 2009.
- [11] IP Zakharov and OA Botsyura. Calculation of expanded uncertainty in measurements using the kurtosis method when implementing a bayesian approach. *Measurement techniques*, 62:327–331, 2019.
- [12] Chao Li, Chen Gong, Qiang He, and Xinwen Hou. Keep various trajectories: Promoting exploration of ensemble policies in continuous control. *Advances in Neural Information Processing Systems*, 36, 2024.
- [13] Hassam Sheikh, Mariano Phielipp, and Ladislau Boloni. Maximizing ensemble diversity in deep reinforcement learning. In *International Conference on Learning Representations*, 2021.
- [14] Shixiang Shane Gu, Timothy Lillicrap, Richard E Turner, Zoubin Ghahramani, Bernhard Schölkopf, and Sergey Levine. Interpolated policy gradient: Merging on-policy and off-policy gradient estimation for deep reinforcement learning. *Advances in neural information processing systems*, 30, 2017.

- [15] Rasool Fakoor, Pratik Chaudhari, and Alexander J Smola. P3o: Policy-on policy-off policy optimization. In *Uncertainty in artificial intelligence*, pages 1017–1027. PMLR, 2020.
- [16] Frans A Oliehoek, Christopher Amato, et al. *A concise introduction to decentralized POMDPs*, volume 1. Springer, 2016.
- [17] Rémi Munos, Tom Stepleton, Anna Harutyunyan, and Marc Bellemare. Safe and efficient off-policy reinforcement learning. *Advances in neural information processing systems*, 29, 2016.
- [18] Peter H Westfall. Kurtosis as peakedness, 1905–2014. *rip*. *The American Statistician*, 68(3):191–195, 2014.
- [19] Alexandros Gabrielsen, Axel Kirchner, Zhuoshi Liu, and Paolo Zagaglia. Forecasting value-at-risk with time-varying variance, skewness and kurtosis in an exponential weighted moving average framework. *Annals of Financial Economics*, 10(01):1550005, 2015.
- [20] Nicola Loperfido. Kurtosis-based projection pursuit for outlier detection in financial time series. *The European Journal of Finance*, 26(2-3):142–164, 2020.
- [21] Jakub Grudzien Kuba, Muning Wen, Linghui Meng, Haifeng Zhang, David Mguni, Jun Wang, Yaodong Yang, et al. Settling the variance of multi-agent policy gradients. *Advances in Neural Information Processing Systems*, 34:13458–13470, 2021.
- [22] Yifan Zang, Jinmin He, Kai Li, Haobo Fu, Qiang Fu, Junliang Xing, and Jian Cheng. Automatic grouping for efficient cooperative multi-agent reinforcement learning. *Advances in Neural Information Processing Systems*, 36, 2024.
- [23] Yonghyeon Jo, Sunwoo Lee, Junghyuk Yeom, and Seungyul Han. Fox: Formation-aware exploration in multi-agent reinforcement learning. In *Proceedings of the AAAI Conference on Artificial Intelligence*, volume 38, pages 12985–12994, 2024.
- [24] Woojun Kim and Youngchul Sung. An adaptive entropy-regularization framework for multi-agent reinforcement learning. In *International Conference on Machine Learning*, pages 16829–16852. PMLR, 2023.
- [25] Jianhao Wang, Zhizhou Ren, Terry Liu, Yang Yu, and Chongjie Zhang. Qplex: Duplex dueling multi-agent q-learning. *arXiv preprint arXiv:2008.01062*, 2020.
- [26] Tuomas Haarnoja, Aurick Zhou, Pieter Abbeel, and Sergey Levine. Soft actor-critic: Off-policy maximum entropy deep reinforcement learning with a stochastic actor. In *International conference on machine learning*, pages 1861–1870. PMLR, 2018.
- [27] Benjamin Eysenbach and Sergey Levine. Maximum entropy RL (provably) solves some robust RL problems. In *International Conference on Learning Representations*, 2022.
- [28] Richard Y Chen, Szymon Sidor, Pieter Abbeel, and John Schulman. Ucb exploration via q-ensembles. *arXiv preprint arXiv:1706.01502*, 2017.
- [29] Michal Pándy, Andrea Agostinelli, Jasper Uijlings, Vittorio Ferrari, and Thomas Mensink. Transferability estimation using bhattacharyya class separability. In *Proceedings of the IEEE/CVF Conference on Computer Vision and Pattern Recognition*, pages 9172–9182, 2022.
- [30] Yifei Lou, Andrei Irimia, Patricio A Vela, Micah C Chambers, John D Van Horn, Paul M Vespa, and Allen R Tannenbaum. Multimodal deformable registration of traumatic brain injury mr volumes via the bhattacharyya distance. *IEEE Transactions on Biomedical Engineering*, 60(9):2511–2520, 2013.
- [31] T. Kailath. The divergence and bhattacharyya distance measures in signal selection. *IEEE Transactions on Communication Technology*, 15(1):52–60, 1967.
- [32] Mikayel Samvelyan, Tabish Rashid, Christian Schroeder De Witt, Gregory Farquhar, Nantas Nardelli, Tim GJ Rudner, Chia-Man Hung, Philip HS Torr, Jakob Foerster, and Shimon Whiteson. The starcraft multi-agent challenge. *arXiv preprint arXiv:1902.04043*, 2019.
- [33] Siqi Shen, Chennan Ma, Chao Li, Wei-quan Liu, Yongquan Fu, Songzhu Mei, Xinwang Liu, and Cheng Wang. Riskq: risk-sensitive multi-agent reinforcement learning value factorization. *Advances in Neural Information Processing Systems*, 36:34791–34825, 2023.
- [34] Zhiwei Xu, Yunpeng Bai, Bin Zhang, Dapeng Li, and Guoliang Fan. Haven: Hierarchical cooperative multi-agent reinforcement learning with dual coordination mechanism. In *Proceedings of the AAAI Conference on Artificial Intelligence*, volume 37, pages 11735–11743, 2023.
- [35] Pengyi Li, Jianye Hao, Hongyao Tang, Yan Zheng, and Xian Fu. Race: improve multi-agent reinforcement learning with representation asymmetry and collaborative evolution. In *International Conference on Machine Learning*, pages 19490–19503. PMLR, 2023.

- [36] Anuj Mahajan, Tabish Rashid, Mikayel Samvelyan, and Shimon Whiteson. Maven: Multi-agent variational exploration. *Advances in neural information processing systems*, 32, 2019.
- [37] Owen Lockwood and Mei Si. A review of uncertainty for deep reinforcement learning. In *Proceedings of the AAAI Conference on Artificial Intelligence and Interactive Digital Entertainment*, volume 18, pages 155–162, 2022.
- [38] Eduard Hofer, Martina Kloos, Bernard Krzykacz-Hausmann, Jörg Peschke, and Martin Woltereck. An approximate epistemic uncertainty analysis approach in the presence of epistemic and aleatory uncertainties. *Reliability Engineering & System Safety*, 77(3):229–238, 2002.
- [39] Gregory Kahn, Tianhao Zhang, Sergey Levine, and Pieter Abbeel. Plato: Policy learning using adaptive trajectory optimization. In *2017 IEEE International Conference on Robotics and Automation (ICRA)*, pages 3342–3349. IEEE, 2017.

Algorithm 1: Action Selection

Input: actor policies $\{\pi_i(a_i|\tau_i; \theta_i)\}_{i=1}^k$, individual Q-functions $\{Q_i^{\phi_i}\}_{i=1}^k$, joint trajectory τ , num_agents, action space sizes $\{M_i\}_{i=1}^k$

Output: Selected actions set \mathbf{a}

for agent $i = 1$ to num_agents **do**

 Get action logits $\bar{z}^i = f_{\theta_i}(\tau_i)$

 Calculate kurtosis over all actions for each agent:

$$\bar{g}_i(\tau_i, \{Q^{\phi_{i,j}}\}_{j=1}^N) = \frac{\sum_{z=1}^{M_i} g_2(\{Q^{\phi_{i,j}}(\tau_i, a_z)\}_{j=1}^N)}{M_i}. \quad (22)$$

 Update action logits according to Eq. 15 and the value of \bar{g}_i

 Select action $a_i \sim \sigma(\bar{z}_j)$ with the updated logits using epsilon greedy policy.

end for

Algorithm 2: Ensemble MIX Algorithm

Input: L (num of episodes), T_{max} (episode length), K (num of agents)

Initialize centralized mixing network Q_{tot}^{ϕ} , for each agent i : ensemble critics $\{Q^{\phi_{i,j}}\}_{j=1}^N$, actor networks $\{\pi_{\theta_i}\}_{i=1}^k$

Initialize target centralized critic $Q_{tot}^{\phi'} = Q_{tot}^{\phi}$, target ensemble critics $Q^{\phi'_{i,j}} = Q^{\phi_{i,j}}$

Initialize on-policy replay buffer \mathcal{D}_{on} , off-policy replay buffer \mathcal{D}_{off}

for episode = 1 to L **do**

 Initialize environment and agents

for $t = 1$ to T **do**

 Observe state s_t

 obtain joint action set \mathbf{a}_t by calling Algorithm 1

 Execute joint actions \mathbf{a}_t

 Receive reward r_t and next state s_{t+1}

 Store transition $(s_t, \mathbf{a}_t, r_t, s_{t+1})$ in replay buffers \mathcal{D}_{on} and \mathcal{D}_{off}

 Sample minibatch N_1 from replay buffer \mathcal{D}_{on}

 Sample minibatch N_2 from replay buffer \mathcal{D}_{off}

 Calculate the Bhattacharyya loss $\delta_{B_{total}}^{Q_i}$ for sampled batches $\{N_2, N_1\}$

 Update the critics with the loss in Eq. 17 using a mix of on-policy and off-policy losses.

 Update decentralized actors using a mix of on-policy and off-policy loss functions (Eq. 13)

if $t \bmod X = 0$ **then**

 Update target networks: $Q^{\phi'_{i,j}} = Q^{\phi_{i,j}}, Q_{tot}^{\phi'} = Q_{tot}^{\phi}$

end if

end for

end for

A Algorithm

The full specifications of our approach are described in Algorithms 1& 2. The main training loop begins in algorithm 2. The learning parameters are initialized at the beginning of the algorithm and the training loop is executed iteratively for X episodes. Action selection is performed in algorithm 1. Note that our proposed exploration is executed when the excess kurtosis is positive, otherwise, a standard epsilon greedy selection is performed. The critics' loss function can be divided into two parts, the Bhattacharyya term which ensures diversity in the ensemble, and the critic loss, which utilizes the weighted Q_{tot} to reduce variance in the centralized critic. Note that both the critics and the actors are trained with a mix of offline and online data. The online data is sampled from a smaller buffer \mathcal{D}_{on} and $|N_2| > |N_1|$.

B Training Parameters and computation resources

Configurations and hyper-parameters values are provided in table 1.

Table 1: Hyperparameter Table - SMAC

Algorithm Parameters	
HyperParameters	Value
T (train interval)	20K
U (num test episodes)	24
C_1	0.01
C_2	0.001
β	0.001
v	0.5
N_1	32
N_2	5000
ensemble size (N)	10

All experiments are conducted on stations with 64 Intel(R) Xeon(R) CPU E5-2683 v4 @ 2.10GHz, 251G RAM, and NVIDIA GeForce GTX 1080 Ti 12GB.

C Starcraft II scenarios

Our main focus is on scenarios that require the agents to learn diverse skills or exhibit some level of exploration to solve the task. We use the term diversity to describe inter-agent diversification, meaning different agents acquiring different sets of skills. Note that then the state space in all SMAC maps is augmented with the unit type, which allows the agents to acquire different roles based on the unit type.

MMM2. Two identical teams battle each other, aiming to eliminate the units of the opposing team. Each team controls 3 types of units. The first type is a flying, healing unit called Medivac, capable of restoring health to nearby units. The second are the Marines units, which are capable of attacking both ground and air enemy units, and third, the Marauders, bulkier units only capable of attacking enemy ground units. The MMM2 scenario requires diversity among agents, where each type of agent needs to learn a different set of strategies.

MMM3 (7m2M1M vs 9m3M1M) . This is a ultra hard version of the MMM2 map. The allies control a smaller team of 10 agents compared to the larger enemy team of 13 agents.

1c3s5z vs 1c3s6z.A scenario where both teams control 3 types of agents, Colossus, Stalkers, and Zealots. The enemy team has a higher number of Zealots.

3s vs 5z. In this scenario, 3 Stalkers (ranged units) are controlled by agents facing 5 Zealots (melee units). The challenge lies in overcoming the numerical disadvantage by leveraging Stalkers’ kiting abilities, coordinating attacks, and maintaining effective positioning to avoid Zealots’ close-range damage.

D Implementation & Reproducibility

All source code will be made available on publication under an open-source license. We refer the reader to the included README file, which contains instructions to recreate the experiments discussed in this paper.

E Epistemic and aleatoric uncertainty in multi-agent RL

In MARL environments, aleatoric uncertainty, or inherent randomness [37], arises from various sources, including the stochastic dynamics of the environment, inherent noise, agents’ stochastic policies (e.g., epsilon-greedy), and policies shift that introduce non-stationarity. Epistemic uncertainty (lack of knowledge [38]), on the other hand, stems from limited familiarity with the environment’s model (e.g., rewards and transitions) or an incomplete understanding of agents’ policies in relation to one another. The presence of multiple agents within the same environment introduces both aleatoric and epistemic uncertainty, as agents’ exploration and stochastic policies induce aleatoric uncertainty [37] and unfamiliarity of agents with other agents’ models and the environment is epistemic.

In our uncertainty-weighted critic, we apply the weighting by utilizing ensemble kurtosis, i.e., disagreement between ensemble members, which is usually associated with epistemic uncertainty. Yet, the noise in our settings stems both sources: randomness in agent policies (i.e., aleatory) and epistemic uncertainty originated from the unfamiliarity of agents with the model of one another. Similar concerns have been addressed by recent works [7], which showed ensemble variability to be effective in capturing aleatoric uncertainty. [7] injected noise into the environment and

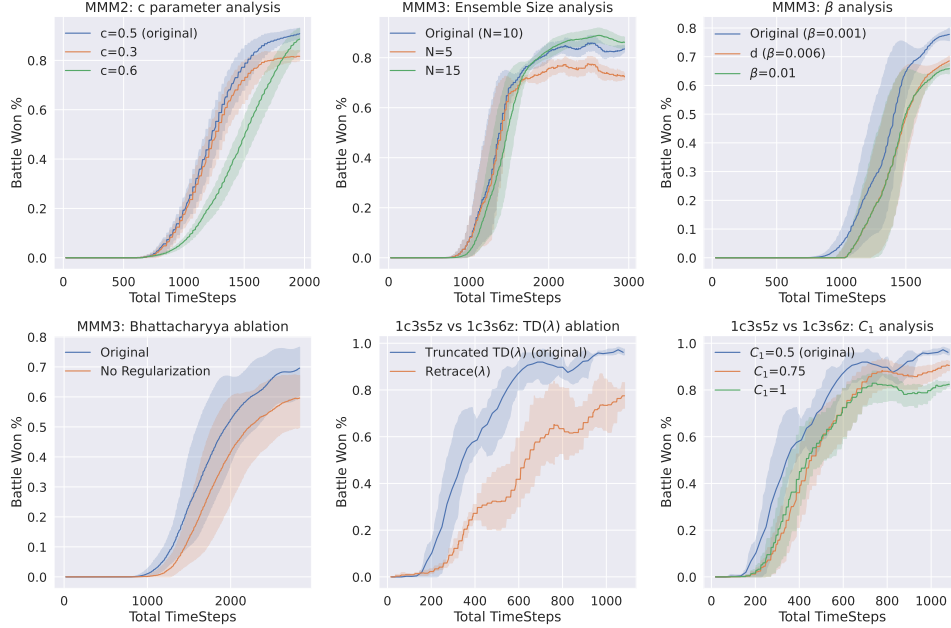


Figure 5: Parameter analysis on MMM2 and MMM3 maps for c , β , C_1 , and ensemble sizes. Ablations on the Bhattacharyya distance and our version of $TD(\lambda)$ versus $retrace(\lambda)$ are presented in the bottom graphs.

detected noisy states via ensemble variability. Motivated by those results, we apply the ensemble approach in our settings, which mixes both epistemic and aleatoric sources.

F Ablation study and parameter analysis

Additional details and results of the ablation study, which were omitted from the main paper, are provided in this section.

Variance versus kurtosis for exploration. In a separate set of experiments, we attempt to use the variance rather than the kurtosis to tune exploration. The process is similar to the algorithm suggested in Section 4.2, but instead of applying it only to high-uncertainty states that correspond to positive excess kurtosis, the variance is added to the actor logits in all time steps, regardless of the level of uncertainty. Note that, unlike kurtosis, where it is custom to use the normal distribution as a reference point, there isn't a similar threshold for the variance. Results are presented in Figure 3 the MMM2 map. It can be seen that kurtosis-based exploration achieves superior results compared to the variance in both scenarios. It is interesting to note that previous studies from the single agent domain which suggested utilizing variance for exploration had more success [7, 28]. We hypothesize the main reason for the difference in performance lies in the transition from the single-agent to the multi-agent domain. Multi-agent systems require the learning algorithm to account for efficiency issues to achieve good results, i.e., when all agents are performing exploration all of the time, it becomes harder to form collaboration due to the large joint action space.

Parameter analysis and additional ablation. Fig. 5 shows analysis with different sizes of β , C_1 , c and varying ensemble size. Ensemble-MIX shows relatively low sensitivity to ensemble size, yet different sizes of β yield greater effect on performances, which is consistent with previous studies that show excessive exploration in multi-agent RL hurts performances. The bottom graphs present ablations on the diversity regularization mechanism and a comparison to the $retrace(\lambda)$ algorithm.

G Theoretical Analysis

The theoretical analysis objective is to bound the bias in the gradient update for each individual agent. Since each agent independently updates its policy, analyzing the bias on a per-agent basis is more intuitive. Our analysis shows that an agent's updates are influenced not only by errors in the approximation of its Q-function but also by other agents' policies.

To derive a bound on the bias we first outline key definitions used in the main paper, beginning with the mixed gradient update:

$$D_\nu^\beta(\pi_i, \pi_{-i}) = (1 - \nu)\mathbb{E}_{\rho^\pi, \pi_i} [\nabla_{\theta_i} \log \pi_i(a_i | \tau_i; \theta_i) U_{\pi_i}^{\phi_i}(\tau_i, a_i)] + \nu\mathbb{E}_{\rho^\beta} [\nabla_{\theta_i} \bar{Q}_{\text{tot}}^\phi(\tau, (a_i, \mathbf{a}_{-i}))], \quad (23)$$

where $\bar{Q}_{\text{tot}}^\phi(\tau, (a_i, \mathbf{a}_{-i})) = \mathbb{E}_{\pi_i} [Q_{\text{tot}}^\phi(\tau, (a_i, \mathbf{a}_{-i}))]$, and ν is the relative scaling factor. The on-policy term in Eq. 23 can be simplified as follows:

$$\mathbb{E}_{\pi_i} [\nabla_{\theta_i} \log \pi_i(a_i | \tau_i) U_{\pi_i}^{\phi_i}(\tau_i, a_i)] \quad (24)$$

$$= \mathbb{E}_{\pi_i} \left[\nabla_{\theta_i} \log \pi_i(a_i | \tau_i) \lambda_i(\tau) \left(Q_i^{\phi_i}(\tau_i, a_i) - \sum_x \pi_i(x | \tau_i) Q_i^{\phi_i}(\tau_i, x) \right) \right] \quad (25)$$

$$= \mathbb{E}_{\pi_i} [\nabla_{\theta_i} \log \pi_i(a_i | \tau_i) \lambda_i(\tau) Q_i^{\phi_i}(\tau_i, a_i)]. \quad (26)$$

Note that the notation $D_\nu^\beta(\pi_i, \pi_{-i})$ has been chosen to distinguish the mixed update from the gradient update of the true objective, which we denote by $\nabla_{\theta_i} J$. To express $\nabla_{\theta_i} J$ we first define the true Q-function of the i_{th} agent [4]:

$$Q_i^\pi(\tau, a_i) = \sum_{\mathbf{a}^{-i}} \pi_{-i}(\mathbf{a}_{-i} | \tau_{-i}) Q_{\text{tot}}^\pi(\tau, (a_i, \mathbf{a}_{-i})), \quad (27)$$

then:

$$\nabla_{\theta_i} J(\pi_i, \pi_{-i}) = \mathbb{E}_{\tau \sim \rho^\pi, \mathbf{a}_i \sim \pi_i} [\nabla_{\theta_i} \log \pi_i(a_i | \tau_i; \theta_i) Q_i^\pi(\tau, a_i)], \quad (28)$$

where $\pi_{-i}(\mathbf{a}_{-i} | \tau_{-i}) = \prod_{j \neq i} \pi_j(a_j | \tau_j)$. The discrepancy between the true Q-function and the weighted approximated Q-function of the i_{th} agent is given by:

$$Q_{\phi_i}^\pi(\tau, a_i) = Q_i^\pi(\tau, a_i) - \lambda_i(\tau) Q_i^{\phi_i}(\tau_i, a_i). \quad (29)$$

We are now ready to prove proposition 1 which gives us a bound on the bias of each agent's updates. To achieve this we measure the difference between the gradient of the true objective $\nabla_{\theta_i} J(\pi_i, \pi_{-i})$ and the mixed gradient update $D_\nu^\beta J(\pi_i, \pi_{-i})$ we use in the paper.

Proposition 1. Let the maximal KL divergence between two policies π, β be denoted by $D_{\max}^{\text{KL}}(\pi, \beta) = \max_{\tau} D_{\text{KL}}(\pi(\cdot | \tau), \beta(\cdot | \tau))$, and let

$\omega_1 = \max_{\tau, \mathbf{a}} \left\| \nabla_{\theta_i} \log(\pi_i(a_i | \tau_i; \theta_i)) \lambda_i(\tau) Q_{\phi_i}^\pi(\tau, a_i) \right\|_1$, $\omega_2 = \max_{\tau} \left\| \nabla_{\theta_i} \lambda_i(\tau) \mathbb{E}_{\pi_i} [Q_i^{\phi_i}(\tau_i, a_i)] \right\|_1$. Then, the learning bias of each agent can be bounded as follows:

$$\left\| \nabla_{\theta_i} J(\pi_i, \pi_{-i}) - D_\nu^\beta(\pi_i, \pi_{-i}) \right\|_1 \leq \frac{\omega_1}{1 - \gamma} + \frac{2\omega_2\nu\gamma}{(1 - \gamma)^2} \sqrt{D_{\max}^{\text{KL}}(\pi, \beta)}. \quad (30)$$

The bound tells us that the bias of each agent's gradient update depends on two main factors: errors in the approximation of Q_i^π , as measured by $Q_{\phi_i}^\pi$, and second, how much the joint on-policy diverge from the (joint) policy used to collect the off-policy data.

Proof. Let the discounted joint state distribution be denoted by:

$$\rho^\pi(\tau) = \sum_{t=0}^{\infty} \gamma^t \rho_t^\pi(\tau), \quad (31)$$

where $\rho_t^\pi(\tau) = p^\pi(\tau_t = \tau)$ denotes the state distribution at time t , following a joint policy π . Then, we can use the following lemma from [39]:

Lemma 1. Let ρ_t^π and ρ_t^β be two state distributions at time t . Then the following bound holds:

$$\|\rho_t^\pi - \rho_t^\beta\|_1 \leq 2t \sqrt{D_{\max}^{\text{KL}}(\pi, \beta)}. \quad (32)$$

Given Lemma 1 we are ready to prove the bound in Proposition 1:

$$\begin{aligned}
& \left\| \nabla_{\theta_i} J(\pi_i, \pi_{-i}) - D_{\nu}^{\beta}(\pi_i, \pi_{-i}) \right\|_1 \\
&= \left\| \mathbb{E}_{\rho^{\pi}, \pi_i} \left[\nabla_{\theta_i} \log \pi_i(a_i | \tau_i; \theta_i) Q_i^{\pi}(\tau, a_i) \right] - (1 - \nu) \mathbb{E}_{\rho^{\pi}, \pi_i} \left[\nabla_{\theta_i} \log \pi_i(a_i | \tau_i; \theta_i) \lambda_i(\tau) Q_i^{\phi_i}(\tau_i, a_i) \right] \right. \\
&\quad \left. - \nu \mathbb{E}_{\rho^{\beta}} \left[\nabla_{\theta_i} \overline{Q}_{\text{tot}}^{\phi}(\tau, (a_i, \mathbf{a}_{-i})) \right] \right\|_1 \\
&\stackrel{(*)}{=} \left\| \mathbb{E}_{\rho^{\pi}, \pi_i} \left[\nabla_{\theta_i} \log \pi_i(a_i | \tau_i; \theta_i) \left(Q_i^{\pi}(\tau, a_i) - \lambda_i(\tau) Q_i^{\phi_i}(\tau_i, a_i) \right) \right] + \nu \mathbb{E}_{\rho^{\pi}, \pi_i} \left[\nabla_{\theta_i} \log \pi_i(a_i | \tau_i; \theta_i) \lambda_i(\tau) Q_i^{\phi_i}(\tau_i, a_i) \right] \right. \\
&\quad \left. - \nu \mathbb{E}_{\rho^{\beta}} \left[\nabla_{\theta_i} \lambda_i(\tau) \mathbb{E}_{\pi_i} [Q_i^{\phi_i}(\tau_i, a_i)] \right] \right\|_1 \\
&\stackrel{(**)}{\leq} \left\| \mathbb{E}_{\rho^{\pi}, \pi_i} \left[\nabla_{\theta_i} \log \pi_i(a_i | \tau_i; \theta_i) \left(Q_i^{\pi}(\tau, a_i) - \lambda_i(\tau) Q_i^{\phi_i}(\tau_i, a_i) \right) \right] \right\|_1 \\
&\quad + \nu \left\| \mathbb{E}_{\rho^{\pi}, \pi_i} \left[\nabla_{\theta_i} \log \pi_i(a_i | \tau_i; \theta_i) \lambda_i(\tau) Q_i^{\phi_i}(\tau_i, a_i) \right] - \mathbb{E}_{\rho^{\beta}} \left[\nabla_{\theta_i} \lambda_i(\tau) \mathbb{E}_{\pi_i} [Q_i^{\phi_i}(\tau_i, a_i)] \right] \right\|_1 \\
&\stackrel{(***)}{\leq} \omega_1 \sum_{t=0}^{\infty} \gamma^t + \nu \omega_2 \sum_{t=0}^{\infty} \gamma^t \left\| \rho_t^{\pi} - \rho_t^{\beta} \right\|_1 \\
&\leq \frac{\omega_1}{1 - \gamma} + 2\nu \omega_2 \left(\sum_{t=0}^{\infty} \gamma^t t \right) \sqrt{D_{\max}^{\text{KL}}(\pi, \beta)} \\
&= \frac{\omega_1}{1 - \gamma} + \frac{2\nu \omega_2 \gamma}{(1 - \gamma)^2} \sqrt{D_{\max}^{\text{KL}}(\pi, \beta)}. \tag{33}
\end{aligned}$$

Transition $(*)$ leverages the additive structure of Q_{tot} by replacing $Q_{\text{tot}}^{\phi}(\tau, (a_i, \mathbf{a}_{-i}))$ with $Q_i^{\phi_i}(\tau, a_i)$, this is allowed since applying the gradient with respect to θ_i cancels out all the components of Q_{tot} that are independent of Q_i . Transition $(**)$ rearranges the terms and utilizes the triangle inequality to separate the original term into 2 different expressions. In transition $(***)$ and onward we bound the bias by taking the maximum value of each expression and extracting ω_1 and ω_2 from the respective sums. The first term is bounded with ω_1 as follows:

$$\begin{aligned}
& \left\| \mathbb{E}_{\rho^{\pi}, \pi_i} \left[\nabla_{\theta_i} \log \pi_i(a_i | \tau_i; \theta_i) \left(Q_i^{\pi}(\tau, a_i) - \lambda_i(\tau) Q_i^{\phi_i}(\tau_i, a_i) \right) \right] \right\|_1 \\
&= \left\| \sum_{t=0}^{\infty} \gamma^t \sum_{\tau} \rho_t^{\pi}(\tau) \sum_{a_i \in \mathcal{A}} \pi_i(a_i | \tau_i; \theta_i) \nabla_{\theta_i} \log \pi_i(a_i | \tau_i; \theta_i) \left(Q_i^{\pi}(\tau, a_i) - \lambda_i(\tau) Q_i^{\phi_i}(\tau_i, a_i) \right) \right\|_1 \\
&\leq \max_{\tau, \mathbf{a}} \left\| \nabla_{\theta_i} \log (\pi_i(a_i | \tau_i; \theta_i)) \lambda_i(\tau) Q_i^{\pi_i}(\tau, a_i) \right\|_1 \sum_{t=0}^{\infty} \gamma^t \sum_{\tau} \rho_t^{\pi}(\tau), \tag{34}
\end{aligned}$$

with $\sum_{\tau} \rho_t^{\pi}(\tau) = 1$ and ω_1 equal the maximum over τ and \mathbf{a} . The second term, which we bound using ω_2 , represents the difference between two distinct mean expressions. To derive a bound, we need to ensure that the same expression appears inside both means. Using the following transition:

$$\nabla_{\theta_i} \log \pi_i(a_i | \tau_i; \theta_i) = \frac{\nabla_{\theta_i} \pi_i(a_i | \tau_i; \theta_i)}{\pi_i(a_i | \tau_i; \theta_i)}, \tag{35}$$

we can write:

$$\begin{aligned}
& \mathbb{E}_{\rho^{\pi}, \pi_i} \left[\nabla_{\theta_i} \log \pi_i(a_i | \tau_i; \theta_i) \lambda_i(\tau) Q_i^{\phi_i}(\tau_i, a_i) \right] \\
&= \mathbb{E}_{\rho^{\pi}, \pi_i} \left[\frac{\nabla_{\theta_i} \pi_i(a_i | \tau_i; \theta_i)}{\pi_i(a_i | \tau_i; \theta_i)} \lambda_i(\tau) Q_i^{\phi_i}(\tau_i, a_i) \right] \\
&= \mathbb{E}_{\rho^{\pi}} \left[\sum_{a_i \in \mathcal{A}} \pi_i(a_i | \tau_i; \theta_i) \frac{\nabla_{\theta_i} \pi_i(a_i | \tau_i; \theta_i)}{\pi_i(a_i | \tau_i; \theta_i)} \lambda_i(\tau) Q_i^{\phi_i}(\tau_i, a_i) \right] \\
&= \mathbb{E}_{\rho^{\pi}} \left[\nabla_{\theta_i} \lambda_i(\tau) \mathbb{E}_{\pi_i} [Q_i^{\phi_i}(\tau_i, a_i)] \right]. \tag{36}
\end{aligned}$$

This gives us the same expression in both means which differ only by state distributions:

$$\begin{aligned}
& \left\| \mathbb{E}_{\rho^\pi} \left[\nabla_{\theta_i} \lambda_i(\boldsymbol{\tau}) \mathbb{E}_{\pi_i} [Q_i^{\phi_i}(\tau_i, a_i)] \right] - \mathbb{E}_{\rho^\beta} \left[\nabla_{\theta_i} \lambda_i(\boldsymbol{\tau}) \mathbb{E}_{\pi_i} [Q_i^{\phi_i}(\tau_i, a_i)] \right] \right\|_1 \\
& \leq \sum_{t=0}^{\infty} \gamma^t \left\| \mathbb{E}_{\rho_t^\pi} \left[\nabla_{\theta_i} \lambda_i(\boldsymbol{\tau}) \mathbb{E}_{\pi_i} [Q_i^{\phi_i}(\tau_i, a_i)] \right] - \mathbb{E}_{\rho_t^\beta} \left[\nabla_{\theta_i} \lambda_i(\boldsymbol{\tau}) \mathbb{E}_{\pi_i} [Q_i^{\phi_i}(\tau_i, a_i)] \right] \right\|_1 \\
& \leq \max_{\boldsymbol{\tau}} \left\| \nabla_{\theta_i} \lambda_i(\boldsymbol{\tau}) \mathbb{E}_{\pi_i} [Q_i^{\phi_i}(\tau_i, a_i)] \right\|_1 \sum_{t=0}^{\infty} \gamma^t \left\| \rho_t^\pi - \rho_t^\beta \right\|_1, \tag{37}
\end{aligned}$$

where the technique for bounding the difference between two means is similar to the proof presented in [14]. \square